Down-Regulation of Amygdala and Insula Functional Circuits by Varenicline and Nicotine in Abstinent Cigarette Smokers

Supplemental Information

Supplemental Text

Supplemental Data

Supplemental Tables

Supplemental References

Supplemental Text

Study Overview

To examine resting-state functional connectivity (rsFC) modulations in accord with our hypothesized PILL x PATCH pharmacological interaction pattern (main text Figure 1), participants completed 6 neuroimaging assessments on separate days over a 5-6 week period (Figure S1). The study physician maintained and randomized drug orders while those collecting data were blinded.

Before beginning a study pill regimen (pre-pill), participants first completed neuroimaging assessments wearing nicotine or placebo patches on separate days. Subsequently, participants underwent varenicline (mean ± SD: 17.0 ± 4.2 days) and placebo pill administration (16.5 ± 3.4 days) and again completed nicotine and placebo patch scans towards the end of each medication period. Varenicline was administered according to standard guidelines: 0.5 mg once daily for days 1-3, 0.5 mg twice daily for days 4-7, and 1 mg twice daily beginning on day 8.

Given a ~24 h elimination half-life (1), and an estimate of 5-6 half-lives for a medication to reach steady state, neuroimaging sessions occurred ~14-17 days after the onset of pill administration. This ~2 week interval served as a titration period to minimize side effects (i.e., nausea and vomiting) and allow drug plasma concentration levels to reach a steady state. To further mitigate the likelihood of encountering physical side effects (i.e., nausea and vomiting), particularly in nonsmokers, all participants performed a nicotine patch "toleration test" before completing additional study procedures. During this toleration test participants were instructed to wear the patch for several hours and were contacted via telephone regarding any side effects. None of the participants that completed the study reported any severe issues with the patch during this toleration test.

Additionally, given varenicline's ~24 h half-life, we assumed varenicline carryover effects were negligible in those participants first receiving active medication as subsequent scanning under placebo pills occurred ~2 weeks after the last active dose. Empirically, when considering the primary circuits of interest (i.e., amygdala-insula and insula-posterior cingulate cortex (PCC)) we did not detect an order (carryover) effect. Specifically, when assessing rsFC in an ORDER (varenicline-pill first vs. placebo-pill first) x PILL (pre- vs. placebo vs. varenicline) x

PATCH (placebo vs. nicotine) mixed-effects analysis of variance (ANOVA), we did not detect any significant ORDER-related effects or interactions (p's > 0.2).

Smokers were instructed to abstain from smoking for 12 h before each visit. Indicative of compliance, smokers' CO levels were lower the morning of neuroimaging days (6.9 ± 2.6 ppm) in comparison to visits not requiring abstinence (18.6 ± 8.9 ppm; $t_{[22]} = -7.8$, $p < 0.001$), whereas nonsmokers' CO did not differ (1.9 ± 0.3 ppm vs. 1.8 ± 0.4 ppm; $t_{[18]} = 1.1$, $p = 0.2$).

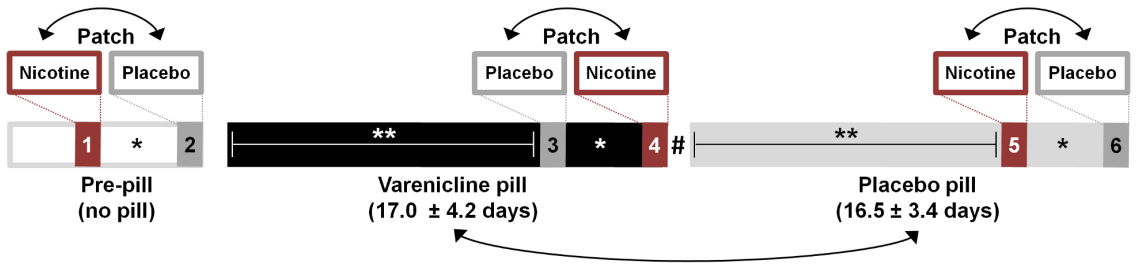

Figure S1. Study overview schematic. Each participant completed six fMRI visits. *Nicotine and placebo patch scans were separated by an average of 2.9 ± 1.7 days. **Neuroimaging assessments occurred 13.9 ± 2.3 days after the onset of each PILL period. # A washout interval did not separate varenicline and placebo pill epochs. Double-headed arrows indicate the randomization of drug order across participants.

Magnetic Resonance Image Collection Parameters

Data were acquired with a Siemens 3T Magnetom Allegra scanner (Erlangen, Germany). 'Resting' data (i.e., in the absence of an externally-cued, performance demanding task) were collected ~2.5-3 h after patch application. Pharmacokinetic data indicate nicotine plasma concentrations reach a peak within 2-4 h after patch application, remain relatively stable for the next 4-6 h, and then gradually decrease beginning ~8-10 h post-patch (2). As such, data collection began ~2.5 h after patch application. During the 8-min resting scan, participants were instructed to simply relax with eyes closed and remain still.

Thirty-three 5-mm thick slices were obtained in the sagittal plane using a T2*-weighted, single-shot gradient-echo, echo-planar imaging sequence sensitive to blood oxygenation level-dependent effects (240 volumes; repetition time [TR] = 2,000 ms [332 ms delay]; echo time [TE] = 27 ms; flip angle [FA] = 80°; field of view = 220 x 220 mm; image matrix = 64 x 64). As simultaneous electroencephalogram data were also obtained (not discussed further), sagittal images were collected with a delay between volume acquisitions to aid scanner-artifact removal

from electroencephalogram recordings. We also acquired sagittal structural images using a 3D magnetization prepared rapid gradient-echo T1-weighted sequence (TR = 2,500 ms; TE = 4.38 ms; FA = 8°; voxel size = 1 mm^3).

rsFC Analyses: Mitigation Of Head Motion Confounds

Participant head motion is a potential confounding factor that can have systematic influence on rsFC measures (3-7). As such, motion-correction parameters were used to remove signals related to head movement as is commonly practiced. Furthermore, we employed two additional strategies to mitigate motion-related confounds, both of which relied on a measure of volume-to-volume displacement. We estimated the displacement of each brain volume relative to the previous volume from the translational (x, y, z) and rotational (α, β, γ) rigid-body motion-correction parameters. Specifically, displacement was calculated as the Euclidean norm of these 6 realignment parameters (displacement = square root $((\Delta x)^2 + (\Delta y)^2 + (\Delta z)^2 + (\Delta\alpha)^2 + (\Delta\beta)^2 + (\Delta\gamma)^2)$, where e.g., $\Delta x = x_{(i-1)} - x_{(i)}$, such that *i* indexes volume number).

Our first strategy to further mitigate motion-related artifacts involved the censoring of volumes associated with large displacement values from subject-level *Z*-image calculations (3, 7). We censored volumes whose displacement was greater than 0.35 mm/^{o} and its immediately preceding volume. Second, we derived a gross measure of motion over the entirety of each scan which was used as a confounding variable in group-level analyses (5). This summary motion metric was calculated by summing displacement values over all scan volumes and dividing by the number of volumes (i.e., mean motion). The censoring (3, 7) and confounding variable approaches (5) both have been shown to separately reduce the influence of head motion on rsFC measures, and we suggest that combining both of these strategies in our assessments further minimizes the influence of motion-related artifact.

Amygdala Functional Localizer Task

To identify the center coordinates for our amygdala seeds we adopted a variant of the amygdala reactivity paradigm (8, 9). On each trial of the task, participants viewed three simultaneously presented stimuli (a trio) and selected one of the two choice items (bottom) matching the target (top). Four blocks of face presentation were interleaved with five blocks of geometric shape presentation. “Face blocks” consisted of six 4 s trials (2, 4, or 6 s inter-trial

interval). On any given trial, individual stimuli constituting each trio were of similar gender and emotional expression (angry, fearful, surprised, or neutral) and participants indicated via a button press which face was identical to the target. Trios were displayed on the screen for a constant 4 s duration. During each session, a total of 24 pseudo-randomly ordered trios were displayed, 12 of each gender and 6 of each emotional expression. Facial stimuli were obtained from a standard set of images (www.macbrain.org). "Shape blocks" consisted of six 4 s trials (2 s inter-trial interval) and involved presentation of ovals and circles.

To identify regions showing differential activity during face versus shape blocks, individual participant's contrast images were averaged across the six sessions and then submitted to a group-level, one-sample *t*-test. We applied a voxel-wise threshold of $p < 10^{-10}$ to the resulting statistical map with a minimum cluster size of 20 voxels. We used this stringent threshold because the blocked-design and session-averaged contrast images led to a large effect size and high statistical power. These procedures yielded group-level functionally defined clusters encompassing the right (3780 mm^3; center of mass [Talairach, mm]: x = 24, y = -6, z = -16) and left amygdala (2727 mm^3; x = -22, y = -4, z = -16). The influence of varenicline and nicotine on task-based amygdala reactivity has been reported elsewhere (10). These center coordinates were used to define the left and right amygdala rsFC seeds in the current report.

rsFC Analyses: Negative Control Analysis (Nonsmoker Drug Effects)

If amygdala/insula circuit dynamics and pharmacological effects thereon are critically associated with nicotine withdrawal, we predicted that no drug-induced rsFC modulations would be observed in a nonsmoker (negative control) group. After computing *Z*-images for each nonsmoker with the same amygdala and insula seeds used for the smokers, we tested this prediction in two ways using a: 1) region of interest (ROI), and 2) whole-brain approach.

First, we extracted nonsmokers' rsFC values from those ROIs showing drug-induced modulations within the smoker group. By applying those ROIs identified in smokers to the independent nonsmoker group, we were able to perform selective analyses without concern regarding circularity (11). We assessed drug effects in nonsmokers using PILL x PATCH repeated-measures ANOVAs 'off-line' in SPSS 17.0 (Chicago, IL). However, this analysis strategy did not allow us to directly compare smokers versus nonsmokers as such an approach

would constitute a circular analysis. These analyses are shown in Figure S3 (amygdala seed) and Figure S4 (insula seed).

Second, to directly examine differential pharmacological effects between groups across the whole-brain, we assessed the impact of the full agonist nicotine (vs. placebo patch) in the absence of varenicline. Theoretically and empirically, the full agonist provides the most robust effects and thus the greatest power to detect group differences at the whole-brain level. For each participant, we computed contrast images of the average difference between nicotine and placebo patch sessions [((NICOTINE$_{\text{pre-pill}}$–PLACEBO$_{\text{pre-pill}}$)+(NICOTINE$_{\text{placebo-pill}}$–PLACEBO$_{\text{placebo-pill}}$))/2] using subject-level *Z*-images derived from the left amygdala and insula seeds. The resulting contrast images were then submitted to separate, second-level analyses testing for GROUP effects. In other words, we assessed the whole-brain GROUP (smoker vs. nonsmoker) x PATCH (nicotine vs. placebo) interaction (controlling for age and motion; $p_{\text{corrected}} < 0.05$). These analyses are shown in the main text Figure 4.

Supplemental Data

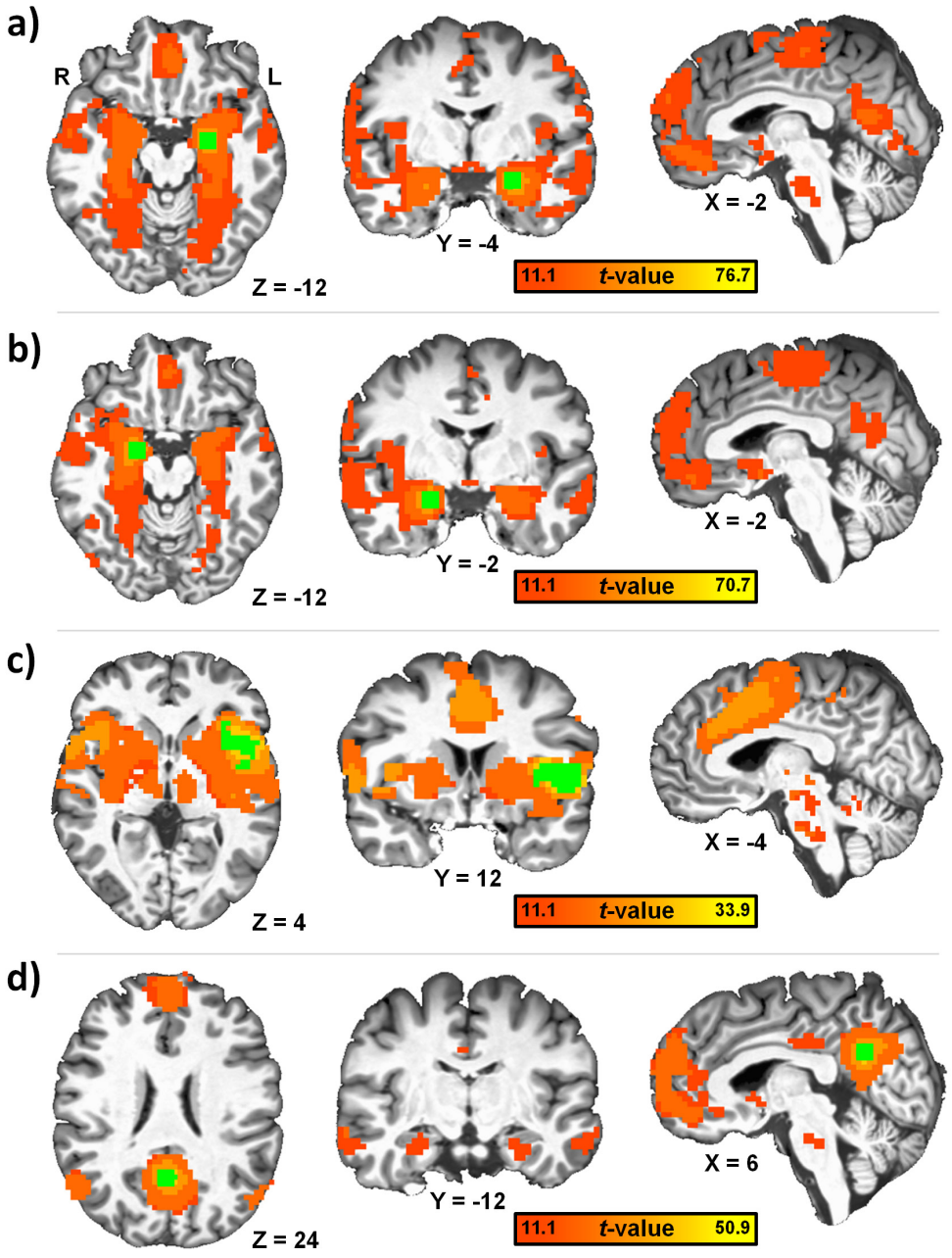

Figure S2. Overall rsFC maps from smokers employing the amygdala, insula, and PCC seeds. We obtained group-level rsFC maps using one-sample *t*-tests performed on session-averaged *Z*-images and, for visualization, applied a voxel-wise threshold of $p < 10^{-11}$. Across all smokers and sessions, the left (**a**) and right amygdala (**b**) seeds (green) identified similar and expected ICNs (12, 13). The left insula seed (**c**) identified an ICN consisting of bilateral insula and posterior medial prefrontal regions, the so-called salience network (14, 15). A seed placed in the PCC (**d**) extracted the canonical default-mode network (16). ICN, intrinsic connectivity network; L, left; PCC, posterior cingulate cortex; R, right; rsFC, resting-state functional connectivity.

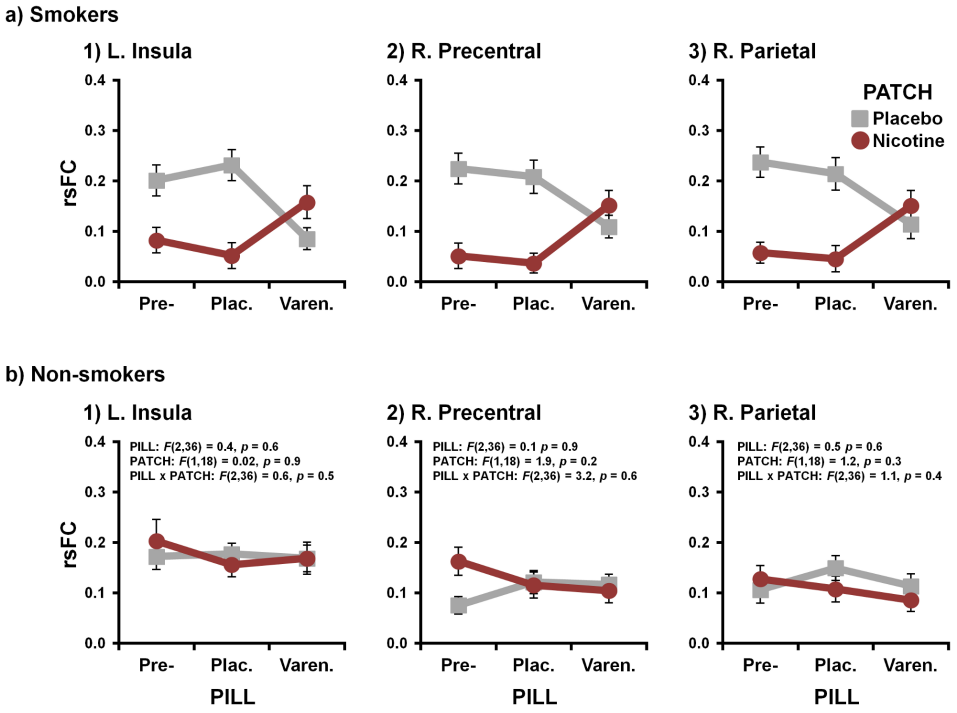

Figure S3. Amygdala-centric rsFC modulations following varenicline and nicotine administration in both smokers and nonsmokers. (**a**) In smokers, drugs reduced the amygdala's rsFC with the left insula, right precentral gyrus, and right superior parietal lobule. Numbering corresponds to shown that in Figure 2A (main text); see Table S1 for coordinates. (**b**) In nonsmokers, there was no evidence that varenicline or nicotine altered rsFC when assessing those ROIs showing drug-induced modulations within the smoker group. Statistics reported are from PILL x PATCH ANOVAs conducted separately for each ROI. Statistics are not reported for smokers as such an approach would constitute a circular analysis (11). L, left; Plac., placebo; R, right; ROI, region of interest; rsFC, resting-state functional connectivity; Varen., varenicline.

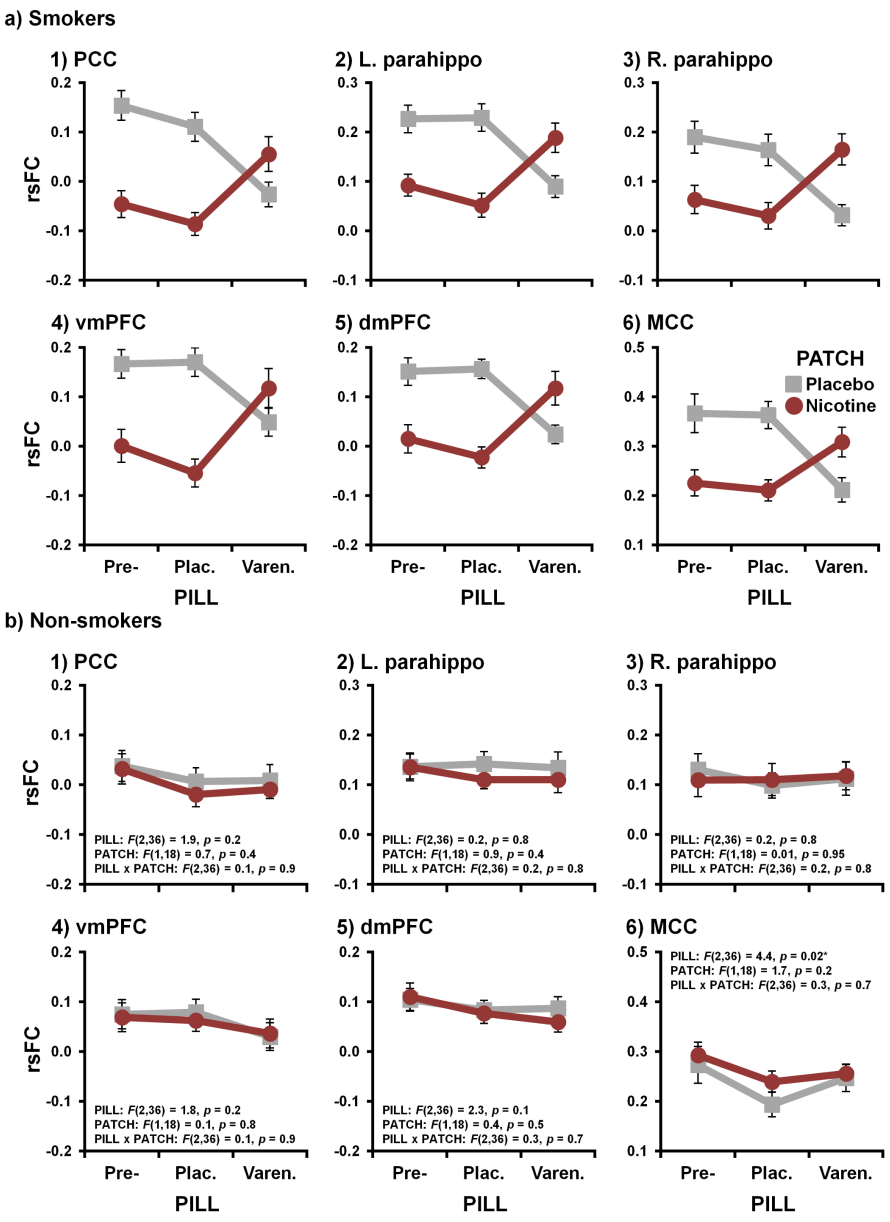

Figure S4. Insula-centric rsFC modulations following varenicline and nicotine administration in both smokers and nonsmokers. (**a**) In smokers, drugs reduced the insula's functional interconnectedness with the PCC/precuneus, bilateral parahippocampus, vmPFC, dmPFC, and MCC. Numbering corresponds to that in Figure 2B (main text); see Table S3 for coordinates. (**b**) In nonsmokers, there was no evidence that varenicline or nicotine altered rsFC when assessing those ROIs showing drug-induced modulations within the smoker group. However, in the MCC ROI a significant PILL main effect was detected ($F_{[2,36]} = 4.4$, $p = 0.02$) such that insula-MCC rsFC was elevated during pre-pill versus placebo-pill conditions ($t_{[18]} = 2.9$, $p = 0.02$) but not when compared with varenicline sessions ($p = 0.4$). As nonsmokers did not receive active medication (i.e., varenicline) during the pre-pill or placebo-pill sessions, this statistically significant difference does not reflect pharmacological effects. Rather the difference in this instance likely reflects novelty/order effects as pre-pill sessions were always the first of the study whereas subsequent visits were randomized. dmPFC, dorsomedial prefrontal cortex; L, left; MCC, mid-cingulate cortex; PCC, posterior cingulate cortex; Plac., placebo; R, right; ROI, region of interest; rsFC, resting-state functional connectivity; Varen., varenicline; vmPFC, ventromedial prefrontal cortex.

rsFC and Subjective and Objective Measures of Withdrawal

We have reported elsewhere (10) that subjective and objective measures of withdrawal severity were reduced by varenicline and nicotine in these abstinent smokers. Subjectively, self-reported withdrawal symptoms (17) were decreased by nicotine (PATCH effect: $p = 0.02$) and as a function of pill-status (PILL effect: $p < 0.001$). Objectively, during performance of the amygdala reactivity task (9) used to functionally-define the amygdala seed coordinates, reaction times (RT) were reduced by drugs in a manner consistent with varenicline's partial agonist profile (PILL x PATCH: $p = 0.01$). In contrast, we did not detect drug-induced changes when assessing Beck Depression Inventory (18), Beck Anxiety Inventory (19), or Positive and Negative Affect Schedule (20) negative affect scores. These null outcomes were likely due to floor effects associated with low scores on these measures, consistent with the argument that our participants were free from psychiatric issues before and during the study.

To relate changes in rsFC with these subjective and objective measures of withdrawal severity, we performed exploratory whole-brain correlation analyses. That is, we used self-reported withdrawal symptoms collected outside the scanner and RTs during subsequent task performance from each smoker and session to separately predict the corresponding session's rsFC values. The resulting whole-brain correlation maps were thresholded at $p_{\text{corrected}} < 0.01$ ($p_{voxel\text{-}wise} < 0.005$; cluster-extent: 86 voxels). Of interest were those brain regions displaying rsFC with the seed region that: 1) were modulated by drugs, and 2) co-varied with self-reports or RT. As such, we created conjunction maps to identify clusters (extent: 10 voxels) surviving threshold in both the correlation and drug effects analyses.

The insula's connectivity strength with the PCC and dorsomedial prefrontal cortex (dmPFC) was both modulated by drugs and positively correlated with self-reported withdrawal (Figure S5a). That is, the more severe the self-reported withdrawal, the greater the coherent activity between the insula and PCC/dmPFC. Additionally, insula's rsFC with PCC, parahippocampus, dmPFC, and ventromedial prefrontal cortex was both modulated by drugs and positively correlated with RT (Figure S5b). That is, the slower the RT during task performance the greater insula's rsFC with default mode network (DMN) regions during the resting scan.

In other words, insula-DMN rsFC was both modulated by drugs and covaried with: 1) self-reports collected several hours later outside of the scanner; and, 2) RT during subsequent task performance. These results suggest that a reduction in the functional interaction between the

insula and DMN regions following nicotinic acetylcholine receptor stimulation may, at least in part, contribute to the amelioration of subjectively experienced withdrawal symptoms and objectively assessed performance deficits. Similar conjunction analyses on amygdala-centric rsFC data failed to identify any clusters showing both drug effects and correlations with withdrawal measures.

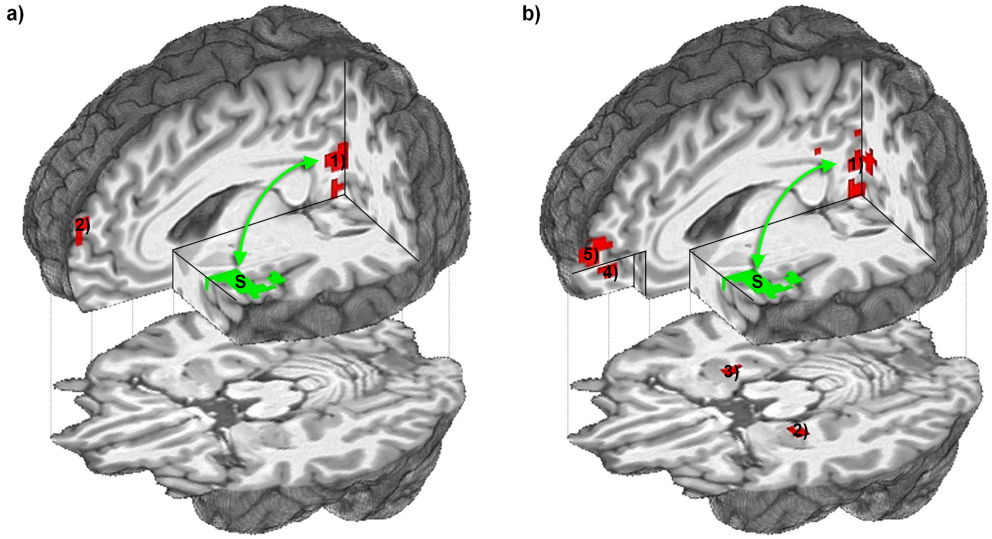

Figure S5. Insula-centric rsFC was associated with subjective and objective measures of withdrawal. Conjunction maps identified regions whose rsFC with an insula seed region (**S**: green) was both modulated by drugs and covaried with self-reported withdrawal symptoms (**a**; PCC: **1**, and dmPFC: **2**) or subsequent task RT (**b**; PCC: **1**, bilateral parahippocampus: **2**, **3**; vmPFC: **4**; and dmPFC: **5**). See Table S3 for coordinates. dmPFC, dorsomedial prefrontal cortex; PCC, posterior cingulate cortex; rsFC, resting-state functional connectivity; RT, reaction time; vmPFC, ventromedial prefrontal cortex.

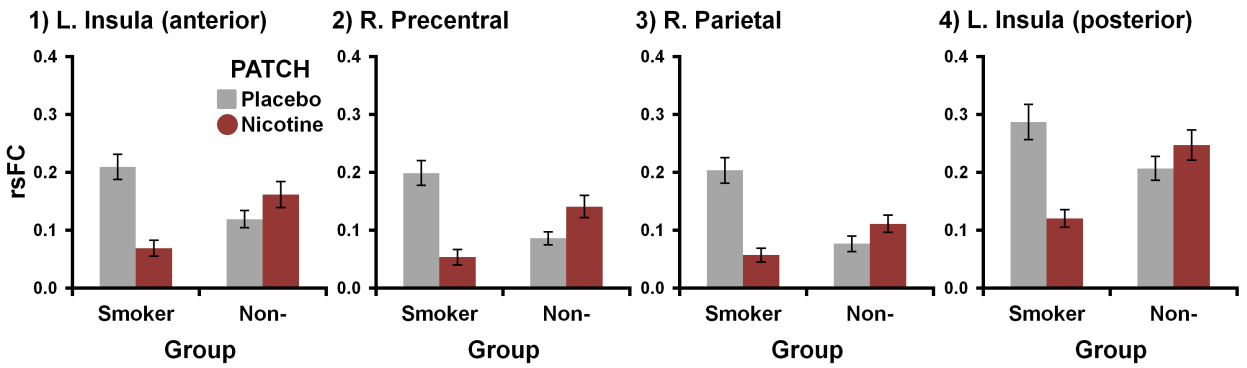

Figure S6. Nicotine-induced decreases in amygdala-centric rsFC were observed in the smoker but not the nonsmoker group. Numbering corresponds to that in Figure 4A (main text); see Table S4 for coordinates. L, left; Non-, nonsmoker; R, right; rsFC, resting-state functional connectivity.

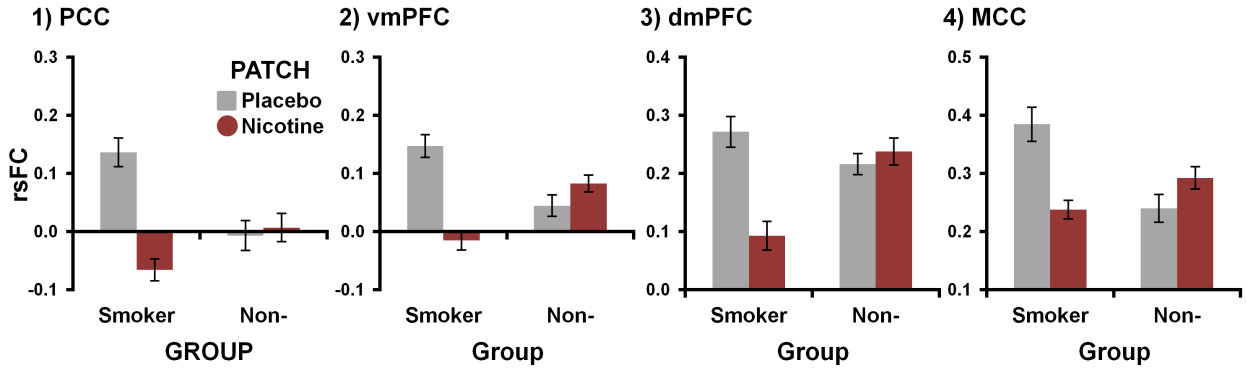

Figure S7. Nicotine-induced decreases in insula-centric rsFC were observed in the smoker but not the nonsmoker group. Numbering corresponds to that in Figure 4B (main text); see Table S5 for coordinates. dmPFC, dorsomedial prefrontal cortex; MCC, mid-cingulate cortex; Non-, nonsmoker; PCC, posterior cingulate cortex; rsFC, resting-state functional connectivity; vmPFC, ventromedial prefrontal cortex.

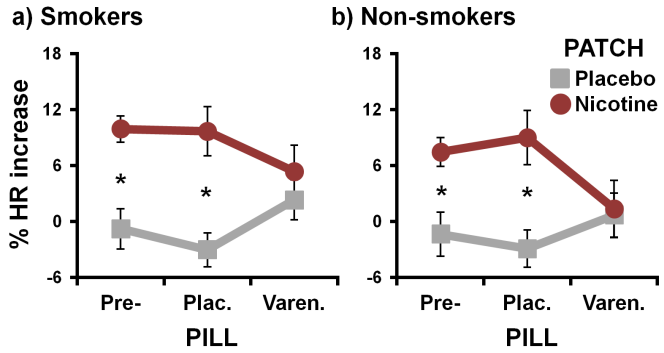

Figure S8. Varenicline and nicotine altered heart rate (HR) in both smokers and nonsmokers. We measured HR each neuroimaging visit before patch application and then at multiple post-patch time points (30, 60, and 120 min). HR values were normalized to percent increase from pre-patch levels and subsequently averaged across post-patch values. Smokers (**a**) and nonsmokers (**b**) displayed similar cardiovascular responses to pharmacological manipulations as indicated by the absence of a GROUP x PILL x PATCH interaction ($p > 0.7$). In both groups, nicotine-induced HR increases were observed under pre-pill and placebo-pill conditions, but not under varenicline conditions (* $p_{corrected} < 0.05$). These results confirm that varenicline and nicotine produced a physiological response in both groups, and despite differences in terms of dose and previous history with nicotine, indicate that smokers and nonsmokers reacted physiologically similar (in terms of HR) to drug manipulations. Additionally, these HR data provide evidence that rsFC alterations observed within smokers were unlikely to be accounted for by general shifts in autonomic tone. That is to say, both smokers and nonsmokers showed alterations in HR, yet only smokers showed rsFC modulations. These HR data have been described in detail elsewhere (10). Plac., placebo; rsFC, resting-state functional connectivity; Varen., varenicline.

Head Motion and rsFC

In general, participant head motion tends to inflate rsFC estimates in local "short-range" circuits and simultaneously, diminish estimates in distributed "long-range" circuits (3-5). Motion confounds persist despite efforts to reduce movement during data collection and commonly employed pre-processing steps (i.e., motion correction and use of realignment parameters as subject-level nuisance regressors) (3). These confounds are of concern because trait or state variation in the ability to remain still may bias rsFC estimates in the direction of hypothesized differences (e.g., neurodevelopmental studies: 3, 4, 5). Thus, there is increasing appreciation that motion should be assessed and accounted for when experimental manipulations may be associated with alterations in head movement during data collection.

To assess session-to-session differences in head movement, we calculated a summary motion metric for each resting scan (mean motion: see Supplemental Text "rsFC analyses: Mitigation of head motion confounds") and analyzed these data in a GROUP (smoker vs.

nonsmoker) x PILL (pre-pill vs. varenicline vs. placebo) x PATCH (nicotine vs. placebo) mixed-effects ANOVA.

We observed that smokers and nonsmokers differed in the degree to which drug administration affected in-scanner head motion as indicated by a GROUP x PATCH interaction ($F_{[1,40]}$ = 6.2, p = 0.02; Figure S9ab). This interaction was driven by a nicotine-induced decrease in motion within the smoker group ($t_{[22]}$ = -4.0, $p_{corrected}$ = 0.002) that was not observed within the nonsmoker group ($t_{[18]}$ = -1.5, $p_{corrected}$ = 0.3). Additional *post hoc* comparisons within the smokers indicated that nicotine administration (vs. placebo patch) decreased motion under all three pill conditions (pre-pill: $t_{[22]}$ = -2.9, $p_{corrected}$ = 0.02; placebo pill: $t_{[22]}$ = -4.0, $p_{corrected}$ = 0.003; varenicline pill: $t_{[22]}$ = -2.6, $p_{corrected}$ = 0.049). In the absence of nicotine, varenicline (vs. placebo pill) administration was also associated with a decrease in motion, albeit non-significant ($t_{[22]}$ = -1.9, $p_{uncorrected}$ = 0.07). Thus, abstinent smokers tended to show reduced in-scanner movement when nicotine (and to a lesser degree, varenicline) was administered.

Briefly summarizing a portion of our main results, nicotine administration to abstinent smokers: 1) decreased "short-range" amygdala-insula rsFC (Euclidean distance = 32.5 mm), 2) decreased "medium-range" insula-PCC rsFC (distance = 64.9 mm), and 3) increased "long-range" PCC-mPFC rsFC (distance = 116.6 mm). While motion's impact on rsFC as a function of inter-regional distance remains to be fully characterized (cf., 3, 5), our pattern of results is close to that expected from a motion-related artifact. In other words, a nicotine-induced decrease in "short-range" (i.e., amygdala-insula) connectivity and an increase in "long-range" (i.e., PCC-mPFC) connectivity could be alternatively explained by reduced movement during those scans when drugs were administered.

To account for motion, we employed three strategies and therefore assume that the drug-induced effects described herein are unlikely fully explained by a movement artifact. First, as is routinely done in rsFC analyses, we used realignment parameters to regress nuisance signals related to residual head motion at the subject-level. Second, the removal of brain volumes associated with large head movements appears to reduce motion's influence on rsFC (3). The percentage of data points censored from the current analyses is presented in Figure S9cd. Third, statistically controlling for movement in group-level analyses by regressing a summary metric as a confounding variable provides an additional approach to account for motion's influence (5). While we employed all three strategies in the current analyses, it is difficult, in general, to

unambiguously separate confounding effects from those of interest. The development of optimal approaches for dealing with motion in rsFC assessments remains an ongoing area of research within the field (6, 7).

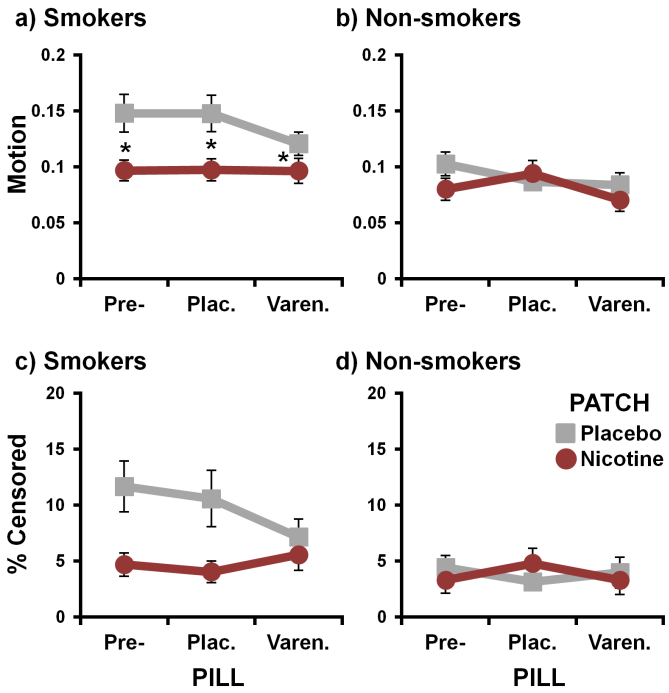

Figure S9. Session-to-session head motion (smokers vs. nonsmokers). A nicotine-induced decrease in mean motion was observed in abstinent smokers (**a**), but not in nonsmokers (**b**). One strategy to mitigate the confounding effects of motion on rsFC, is to censor volumes associated with large head movements from analysis (3). Across all participants and sessions, 5.6% ± 0.7% (mean ± SEM) of the volumes collected were censored (i.e., their displacement was > 0.35 mm/º). The percent of censored volumes is displayed for smokers (**c**) and nonsmokers (**d**). Plac., placebo; rsFC, resting-state functional connectivity; Varen., varenicline.

Supplemental Tables

Table S1. Regions showing drug-induced rsFC modulations with the left amygdala in abstinent smokers.

Region	Hemisphere	Center Coordinates (Talairach)			Cluster size (voxels)
		x	y	z	
PILL x PATCH interaction*					
1) insula	L	-42	12	4	111
2) precentral gyrus	R	34	-6	56	94
3) superior parietal lobule	R	36	-46	60	56
inferior parietal lobule	R	60	-26	32	51

Seed region: left amygdala (x = -22, y = -4, z = -16; 29 voxels). PILL x PATCH interaction: $p_{\text{corrected}} < 0.05$ ($p_{\textit{voxel-wise}} < 0.005$; cluster-extent: 46 voxels).

* Numbering corresponds to that in Figure 2A (main text) and Figure S3.

At an uncorrected threshold ($p_{\textit{voxel-wise}} < 0.005$), a right insula ROI was also observed (x = 38, y = 16, z = 8; 25 voxels).

Region labels come from the AFNI Talairach daemon atlas. Voxel size: 3 x 3 x 3 mm (27 µL).

L, left; R, right; ROI, region of interest; rsFC, resting-state functional connectivity.

Table S2. Regions showing drug-induced rsFC modulations with the right amygdala in abstinent smokers.

Region	Hemisphere	Center Coordinates (Talairach)			Cluster size (voxels)
		x	y	z	
PILL x PATCH interaction					
insula	L	-42	12	8	49
precentral gyrus	R	34	-14	64	119
superior parietal lobule	R	36	-52	60	51
medial frontal gyrus (SMA)	R,L	0	-14	56	54
postcentral gyrus	R	54	-22	38	47

Seed region: right amygdala (x = 24, y = -6, z = -16; 29 voxels). PILL x PATCH interaction: $p_{\text{corrected}} < 0.05$ (voxel-wise: $p < 0.005$; cluster-extent: 46 voxels).

At an uncorrected threshold ($p_{\textit{voxel-wise}} < 0.005$), a right insula ROI was also observed (x = 40, y = 18, z = 6; 40 voxels).

L, left; R, right; ROI, region of interest; rsFC, resting-state functional connectivity; SMA, supplementary motor area.

Table S3. Regions showing drug-induced rsFC modulations with the left insula and correlations with subjective and objective measures of withdrawal severity in abstinent smokers.

Region	Hemisphere	Center Coordinates (Talairach) x	y	z	Cluster size (voxels)
PILL x PATCH interaction (Drugs)*					
1) posterior cingulate/precuneus	R,L	2	-54	26	631
2) parahippocampal gyrus	L	-28	-16	-14	93
3) parahippocampal gyrus	R	32	-20	-14	66
4) anterior cingulate (vmPFC)	R,L	2	40	-8	156
5) superior frontal gyrus (dmPFC)	R,L	-10	60	16	197
6) cingulate gyrus (MCC)	R,L	2	-2	30	53
superior parietal lobule	R	32	-70	46	57
precentral gyrus	R	30	-12	58	53
superior temporal gyrus	R	56	-60	22	35
Withdrawal Correlation					
posterior cingulate/precuneus	R,L	-2	-54	20	84
medial frontal gyrus (dmPFC)	R,L	0	54	20	146
superior frontal gyrus (dlPFC)	L	-36	38	30	164
middle frontal gyrus	L	-44	8	32	141
insula	L	-34	10	4	93
Overlap (Drugs and Withdrawal)**					
1) posterior cingulate/precuneus	R,L	-2	-54	20	65
2) superior frontal gyrus (dmPFC)	L	-10	62	24	22
RT Correlation					
posterior cingulate/precuneus	R,L	2	-62	24	405
medial prefontal cortex	R,L	2	20	30	2685
parahippocampal gyrus	R	26	-26	-20	268
parahippocampal gyrus	L	-24	-32	-16	234
superior temporal gyrus	R	54	-56	26	208
lingual gyrus	R	4	-90	-12	86
Overlap (Drugs and RT)***					
1) posterior cingulate	R,L	-8	-54	22	51
2) parahippocampal gyrus	L	-26	-16	-14	20
3) parahippocampal gyrus	R	30	-20	-14	22
4) medial frontal gyrus (vmPFC)	R	6	50	-4	10
5) medial frontal gyrus (dmPFC)	R,L	-10	62	12	79
posterior cingulate	R,L	4	-44	32	28
precuneus	R,L	2	-64	38	48
superior temporal gyrus	R	56	-62	24	24

Seed region: left insula (x = -42, y = 12, z = 4; 111 voxels). PILL x PATCH interaction (Drug effects): $p_{corrected} < 0.01$ (voxel-wise: $p < 0.001$; cluster-extent: 33 voxels); *Numbering corresponds to that in Figure 2B (main text) and Figure S4.

Withdrawal Correlation: Whole-brain correlation between self-reported withdrawal symptoms and insula-centric rsFC, $p_{corrected} < 0.001$ ($p_{voxel\text{-}wise} < 0.005$; cluster-extent: 86 voxels).

Overlap (Drugs and withdrawal): Conjunction of the two previous analyses (extent threshold: 10 voxels); **Numbering corresponds to that in Figure S5a.

RT Correlation: Whole-brain correlation between task RT and amygdala-centric rsFC.

Overlap (Drugs and RT): Conjunction of Drug effects and RT correlation analyses; ***Numbering corresponds to that in Figure S5b.

dlPFC, dorsolateral prefrontal cortex; dmPFC, dorsomedial prefrontal cortex; L, left; MCC, mid-cingulate cortex; R, right; rsFC, resting-state functional connectivity; RT, reaction time; vmPFC, ventromedial prefrontal cortex.

Table S4. Regions showing differential nicotine-induced rsFC modulations with the left amygdala across GROUP (smokers vs. nonsmokers).

Region	Hemisphere	Center Coordinates (Talairach)			Cluster size (voxels)
		x	y	z	
GROUP x PATCH interaction*					
1) insula	L	-32	20	0	34
2) precentral gyrus	R	32	-6	56	284
3) inferior parietal lobule	R	38	-46	42	838
4) insula (posterior)	L	-44	-6	4	43
precentral gyrus	L	-40	0	42	306
superior parietal lobule	L	-26	-58	50	124
middle frontal gyrus	L	-42	34	18	138
superior frontal gyrus	R	34	50	22	48
cingulate gyrus	R,L	0	-8	42	84
fusiform gyrus	L	-26	-58	-16	86
fusiform gyrus	R	30	-56	-18	37
cuneus	L	-22	-76	32	72
Inferior temproal gyrus	R	56	-58	-8	57

Seed region: left amygdala (x = -22, y = -4, z = -16; 29 voxels). GROUP x PATCH interaction: $p_{\text{corrected}} < 0.05$ ($p_{voxel\text{-}wise} < 0.001$; cluster-extent: 26 voxels). *Numbering corresponds that in Figure 4A (main text) and Figure S6.
L, left; R, right; rsFC, resting-state functional connectivity.

Table S5. Regions showing differential nicotine-induced rsFC modulations with the left insula across GROUP (smokers vs. nonsmokers).

Region	Hemisphere	Center Coordinates (Talairach)			Cluster size (voxels)
		x	y	z	
GROUP x PATCH interaction*					
1) posterior cingulate/precuneus	R,L	2	-52	34	126
2) medial frontal gyrus (vmPFC)	R,L	-4	36	-12	152
3) medial frontal gyrus (dmPFC)	R,L	-2	44	32	50
4) cingulate gyrus (MCC)	R,L	2	-2	32	62
middle frontal gyrus	R	28	26	46	50
medial frontal gyrus	R	2	-14	70	41
precentral gyrus	R	38	-10	60	38
insula (posterior)	L	-44	-8	2	29
posterior cingulate	R	10	-56	14	28
middle temporal gyrus	L	-48	-66	16	31

Seed region: left insula (x = -42, y = 12, z = 4; 111 voxels). GROUP x PATCH interaction: $p_{\text{corrected}} < 0.05$ ($p_{\textit{voxel-wsie}} < 0.001$; cluster-extent: 26 voxels). *Numbering corresponds to that in Figure 4B (main text) and Figure S7.

dmPFC, dorsomedial prefrontal cortex; L, left; MCC, mid-cingulate cortex; R, right; rsFC, resting-state functional connectivity; vmPFC, ventromedial prefrontal cortex.

Supplemental References

1. Faessel HM, Gibbs MA, Clark DJ, Rohrbacher K, Stolar M, Burstein AH (2006): Multiple-dose pharmacokinetics of the selective nicotinic receptor partial agonist, varenicline, in healthy smokers. *J Clin Pharmacol*. 46:1439-1448.

2. Palmer KJ, Buckley MM, Faulds D (1992): Transdermal nicotine - A review of Its pharmacodynamic and pharmacokinetic properties, and therapeutic efficacy as an aid to smoking cessation. *Drugs*. 44:498-529.

3. Power JD, Barnes KA, Snyder AZ, Schlaggar BL, Petersen SE (2012): Spurious but systematic correlations in functional connectivity MRI networks arise from subject motion. *Neuroimage*. 59:2142-2154.

4. Van Dijk KRA, Sabuncu MR, Buckner RL (2012): The influence of head motion on intrinsic functional connectivity MRI. *Neuroimage*. 59:431-438.

5. Satterthwaite TD, Wolf DH, Loughead J, Ruparel K, Elliott MA, Hakonarson H, *et al.* (2012): Impact of in-scanner head motion on multiple measures of functional connectivity: Relevance for studies of neurodevelopment in youth. *Neuroimage*. 60:623-632.

6. Carp J (2012): Optimizing the order of operations for movement scrubbing: Comment on Power et al. *Neuroimage*. http://dx.doi.org/10.1016/j.neuroimage.2011.1012.1061.

7. Power J, Barnes K, Snyder A, Schlaggar B, Petersen S (in press): Steps toward optimizing motion artifact removal in functional connectivity MRI; A reply to Carp. *Neuroimage*. http://dx.doi.org/10.1016/j.neuroimage.2012.1003.1017.

8. Hariri AR, Tessitore A, Mattay VS, Fera F, Weinberger DR (2002): The amygdala response to emotional stimuli: A comparison of faces and scenes. *Neuroimage*. 17:317-323.

9. Bigos KL, Pollock BG, Aizenstein HJ, Fisher PM, Bies RR, Hariri AR (2008): Acute 5-HT reuptake blockade potentiates human amygdala reactivity. *Neuropsychopharm*. 33:3221-3225.

10. Sutherland MT, Carroll AJ, Salmeron BJ, Ross TJ, Hong LE, Stein EA (in press): Individual differences in amygdala reactivity following nicotinic receptor engagement in abstinent smokers. *Neuroimage*. DOI:10.1016/j.neuroimage.2012.10.043.

11. Kriegeskorte N, Simmons WK, Bellgowan PSF, Baker CI (2009): Circular analysis in systems neuroscience: The dangers of double dipping. *Nat Neurosci*. 12:535-540.

12. Roy AK, Shehzad Z, Margulies DS, Kelly AMC, Uddin LQ, Gotimer K, *et al.* (2009): Functional connectivity of the human amygdala using resting state fMRI. *NeuroImage*. 45:614-626.

13. Kim MJ, Gee DG, Loucks RA, Davis FC, Whalen PJ (2010): Anxiety dissociates dorsal and ventral medial prefrontal cortex functional connectivity with the amygdala at rest. *Cereb Cortex*. 21:1667-1673.

14. Seeley WW, Menon V, Schatzberg AF, Keller J, Glover GH, Kenna H, *et al.* (2007): Dissociable intrinsic connectivity networks for salience processing and executive control. *J Neurosci*. 27:2349-2356.

15. Menon V (2011): Large-scale brain networks and psychopathology: a unifying triple network model. *Trends Cog Sci*. 15:483-506.

16. Raichle ME, MacLeod AM, Snyder AZ, Powers WJ, Gusnard DA, Shulman GL (2001): A default mode of brain function. *PNAS*. 98:676-682.

17. Hughes JR, Hatsukami D (1986): Signs and symptoms of tobacco withdrawal. *Arch Gen Psych.* 43:289-294.

18. Beck AT, Steer RA, Ball R, Ranieri WF (1996): Comparison of Beck Depression Inventories-IA and -II in psychiatric outpatients. *J Personality Assessm*. 67:588-597.

19. Beck AT, Brown G, Epstein N, Steer RA (1988): An inventory for measuring clinical anxiety - Psychometric properties. *J Consult and Clin Psychol*. 56:893-897.

20. Watson D, Clark LA, Tellegen A (1988): Development and validation of brief measures of positive and negative affect: The PANAS Scales. *J Personal and Soc Psych*. 54:1063-1070.